Control of Semicontinuous Emulsion Copolymerization Reactors

Enrique Saldívar and W. Harmon Ray
University of Wisconsin—Madison, Madison, WI 53706

The problem of simultaneous control of composition and molecular weight of copolymers produced in semicontinuous emulsion polymerization is addressed. A first-principles model of emulsion copolymerization is used to produce optimal open-loop policies, which are then experimentally tested on the system methyl methacrylate/vinyl acetate. In contrast to earlier work in the control of semicontinuous emulsion copolymerization, the control problem addressed has multiple inputs and multiple outputs, and the experimental application is free of empirical correlations and performed on an unseeded system. Optimal open-loop policies are calculated efficiently by optimizing properties of the instantaneous polymer being formed. The experimental results confirm the feasibility of these techniques. A model-predictive control scheme, in which optimal policies are recomputed on-line to account for disturbances, is proposed. The scheme, which exploits the advantages of the efficient calculation of optimal policies, is tested by simulation showing good performance.

Introduction

The production of emulsion copolymers by batch and semibatch processes is of significant industrial importance. In many cases the amount of material that must be produced does not justify the use of a continuous process and then batch operation is preferred. However, due to the nonsteady nature of batch processes, and to the different rates of reaction of the monomers in a recipe, these processes will produce copolymers whose properties change with the progress of the reaction. The instantaneous copolymer produced will exhibit a drift in copolymer composition and molecular weight. The end result is that the final copolymer, which is a blend of all the copolymers produced instantaneously, will be heterogeneous. Copolymers having the same global composition, but different distribution of composition will have different properties (Ríos et al., 1985; Chujo et al., 1969; El-Aasser et al., 1983). For example, homogeneous emulsion copolymers of vinyl acetate/butyl acrylate will have better adhesive properties than their heterogeneous counterpart (Chujo et al., 1969), so in most practical situations it is desirable to produce homogeneous copolymers. An obvious remedy to this problem is the use of semibatch operation in which flow rates for some of the reactants are introduced in order to nullify the drift in composition and molecular weight. Also, for realistic applications the produced copolymers have to simultaneously satisfy target values on several properties; however, although many studies have been published addressing individually the problems of producing constant composition copolymers by emulsion polymerization or the control of molecular-weight distribution (MWD) in free-radical polymerization, very few works have been published dealing with the problem of multiobjective optimization.

Several researchers have used methods of different degrees of sophistication to obtain constant-composition copolymers. Early works in this area were published by Basset and Hoy (1981) who proposed the power-feed method, and by Guyot et al. (1981), who used an on-line GC and a controller to keep constant the monomer ratio in the feed. Models have been used in conjunction with on-line measurements, on-line state estimation, and feedback control to correct the copolymer composition (Dimitratos et al., 1989 and 1991; Gagnon and MacGregor, 1991; Leiza et al., 1993). Similarly, on-line model calculations and density measurements were used to implement open-loop policies of monomer feed based on conversion instead of time as independent variable (Canegallo et al., 1994; Canu et al., 1994). Another strategy that has been used (Arzamendi and Asúa, 1990; Arzamendi et al., 1991; van Doremaele et al., 1992) is an iterative process that uses empirical correlations to account for model mismatch and unknown parameters in synthesizing optimal monomer feed policies. In these works it has also been shown that monomer-starved processes are more inefficient than processes that use open-loop optimal policies. Starved-condition processes require reaction times considerably longer than the optimal-policies processes to produce copolymers of comparable homogeneity.

Several studies have been published for the optimal control of MWD in the case of free-radical polymerization in solution or bulk (cf. Hicks et al., 1969; Thomas and Kiparissides, 1984; Sacks et al., 1973). In most of them, the maximum principle of Pontryagin (see Ray, 1989) was used to get either maximum or minimum polydispersity or some target values of MWD averages. This technique results in a two-point boundary-value problem (TPBVP), which is difficult to solve.

Only a few works have been published on multivariable control in general free-radical copolymerization (Tsoukas et al., 1982; Congalidis et al., 1989; Choi and Butala, 1991), and only one is known to the authors in emulsion copolymerization (Kozub and MacGregor, 1992).

Open-loop optimal policies that are based on keeping constant the composition of the instantaneous copolymer produced (which we will refer to as instantaneous property technique) have been discussed elsewhere (Broadhead et al., 1985; Arzamendi and Asúa, 1989). The original idea for the control of free-radical copolymerization can be traced back to Hanna (1957). These ideas can also be applied in the multivariable case to simultaneously tailor more than one copolymer property, as shown by Kozub and MacGregor (1992); however, no experimental studies have been published so far for more than one controlled output.

In this article we propose a methodology that uses a detailed first-principles model of emulsion copolymerization to synthesize, via the instantaneous property technique, optimal open-loop monomer and chain transfer agent (CTA) flows to obtain copolymers with constant composition and molecular weight (MW). By using a model of the process, the input/output interactions are automatically taken into account and compensated for to efficiently achieve the control objectives. The feasibility of the techniques is tested by experimental application to the system methyl methacrylate/vinyl acetate. Also, a nonlinear model-predictive control (MPC) scheme, which uses the instantaneous property technique to recompute optimal trajectories on-line in order to account for disturbances, is proposed and tested by simulation. For the MPC scheme a sufficient number of on-line measurements and on-line state estimations are assumed to be available.

As shown later, the synthesis of optimal open-loop policies using this method only requires the solution of the model equations in which the material (or energy) balances for the manipulated variables are replaced by algebraic equations that represent conditions imposed on instantaneous polymer properties. This results in a simpler, more robust method to synthesize open-loop trajectories than the traditional optimal control techniques. This also enhances the feasibility of on-line application, thanks to the speed and reliability of the computations involved. Finally, the calculations can be naturally incorporated into an MPC scheme for on-line recomputation of trajectories in order to deal with disturbances.

In comparing this work to previous ones that have addressed the problem of obtaining optimal trajectories for emulsion copolymerization with experimental verification, two main differences are found: (1) only one variable (composition) was optimized in earlier works; in this article the more realistic multivariable problem is addressed; and (2) previous works have used seeded polymerizations that reduce variability, but that require an additional step in the process; in this work *ab initio* polymerizations are used.

In the next section a systematic methodology for tailoring copolymer properties is introduced, and then the experimental system chosen to test the feasibility of the techniques used is described. The following section addresses the mathematical model used and the efficient generation of optimal open-loop policies. The next section discusses the experiments for parameter estimation and for validation of the synthesized policies with application to the production of copolymers of methyl methacrylate/vinyl acetate with constant composition and molecular weight. Finally, a nonlinear model-predictive control technique based on the on-line recomputation of open-loop optimal policies, is introduced and tested by simulation.

Methodology for Tailoring Copolymer Properties

The methodology proposed comprises the following stages:

- Construction of a mathematical model completely based on first principles (as opposed to partially empirical models) that represents as accurately as possible the emulsion copolymerization process variables and the quality of the polymer produced.
- Design and execution of experiments to estimate unknown parameters of the model.
- Synthesis of optimal open-loop policies based on imposing conditions on the structure of the *instantaneous* polymer formed, as opposed to the use of computationally intensive and more difficult techniques based on optimal control theory (application of Pontryagin maximum principle).
- Experimental verification of optimal open-loop trajectories.
- Implementation of optimal open-loop trajectories aided by a nonlinear MPC scheme, to account on-line for erroneous initial conditions and disturbances. MPC is a natural choice for using the simplified techniques of synthesis of open-loop trajectories mentioned two steps above. In the MPC implementation, the open-loop trajectories are applied only in the relatively small time interval between samples.

Experimental Systems

Chemical system

The system selected to test the optimal control policies developed in this chapter is the emulsion copolymerization of methyl methacrylate (MMA, or monomer 1)/vinyl acetate (VAc, or monomer 2), with chloroform ($CHCl_3$) as chain transfer agent. The system shows widely different reactivity ratios: $r_1 = 20$, $r_2 = 0.015$ (Odian, 1981); which leads to an important drift in composition, and it possesses very different rate coefficients for transfer to monomer and transfer to CTA for each one of the monomers (see Table 1). These facts contribute to make the problem of control of MW a difficult one for this system.

Table 1. Ratios of Transfer to Monomer (C_M) and Transfer to $CHCl_3$ (C_T) to Propagation Rate Coefficients

Monomer	$C_M \times 10^4$	$C_T \times 10^4$
MMA	0.07–0.25*	0.45–1.77**
VAc	1.75–2.8*	125–170**

*Odian, 1981.
**Brandrup and Immergut, 1989.

VAc exhibits transfer-to-polymer (TTP) and terminal double-bond (TDB) polymerization reactions that may significantly affect the MW of the polymer, leading to branching and even gelation.

The goal of the experiments performed was to obtain copolymer with a constant molar composition (50%) and constant weight-average MW along the course of the semicontinuous reaction.

Equipment, materials, and methods

Two different reactor systems were used in these experiments. In the first set of experiments (1–8), which includes the exploratory experiments (1–4), and some of the parameter-fitting experiments (5–8), a glass reactor system described elsewhere (Saldívar and Ray, 1997) was used. In the semicontinuous experiments of this set, peristaltic pumps were used. For the rest of the experiments (9–12), a stainless-steel reactor system with more accurate piston-metering pumps for the feed was used.

The stainless-steel reactor system used for experiments 9–12 consists of a 2.4-L TDH Mfg. Inc. reactor specified and mounted by O. Araujo (1997). The reactor has a magnetic stirrer with a 4-blade turbine impeller working at 254 rpm. A glass condenser can be connected in one of the reactor ports. Two Eldex metering pumps with variable flows controlled by computer were used to feed chloroform and monomer to the reactor. The temperature control was achieved by using a water bath with a centrifugal circulation pump and a CN76000 Omega controller. The temperature was controlled at ±0.5°C of the setpoint. The semicontinuous operation of this system is similar to the one described before (Saldívar and Ray, 1997) except for the fact that all the reactants were charged to the reactor through the condenser port. A complete description of this experimental setup and its operation can be found in Araujo (1997).

Methyl methacrylate monomer from Aldrich (99% purity) and vinyl acetate from Aldrich (+99% purity) were distilled under vacuum at 29″ Hg to remove the inhibitor and other impurities, and then stored in a refrigerator until used a few days later. Potassium persulfate (Aldrich +99% purity) was used as initiator, and sodium dodecyl sulfate (BDH Laboratories, 99%) as emulsifier; both were used without further purification. Chloroform (Aldrich, 99.8% purity, stabilized with 0.5–1% of ethanol) was used as chain transfer agent as received. Nitrogen (Liquid Carbonic, 99.99%) was used for oxygen purging and for keeping an inert atmosphere in the reactor. Deionized water purified by a Millipore filtration system was used in all the reactions. Hydroquinone (Aldrich 99%) was used as inhibitor to stop the reaction in the emulsion samples. The measurement of conversion was done by gravimetric analysis. The copolymer composition was determined by proton Nuclear Magnetic Resonance ^{1}H-NMR.

The measurement of molecular weight was done using viscometry in an Ubbelohde-type Schott-Geräte capillary viscometer. Since Mark-Houwink coefficients were not found in the literature for this copolymer, the corresponding values were estimated using the correlations provided in Van Krevelen (1990) based on additive-group contributions, in which the composition effect can be explicitly accounted for. The estimated Mark-Houwink coefficients (a, K), through Eq. 1, provided values for the viscosity average molecular weight M_v, which were correlated with the weight average value using a constant multiplicative factor:

$$[\eta] = K M_v^a. \tag{1}$$

Mathematical Model and the Instantaneous Property Method

Mathematical model

The mathematical model that was used for control purposes is based on the detailed model presented in Saldívar et al. (1997). The original model, that used partial differential equations (PDEs) to represent the particle-size distribution (PSD) and the moments of the MWD, was reduced by lumping the polymer mass distributed equations (for particle population and MW description) into an average-size (average polymer mass) particle version. A summary of the lumped version resulting equations is presented in the Appendix.

The resulting model contains 18 states: 3 states for the monomer partitioning (see Saldívar et al., 1997); 4 states for monomer/polymer balances; 6 states for balances of other species or global quantities: surfactant, initiator, CTA, water, aqueous phase radicals, and total mass; 2 states for total number of particles and average polymer mass of particles; and 3 states for molecular weight moments.

Synthesis of optimal open-loop policies

The instantaneous property technique maintains constant properties in the polymer by forcing the invariance of corresponding properties in the instantaneous polymer being formed. This is done by solving simultaneously the algebraic equations that force the instantaneous polymer properties to the desired constant values of the output variables, together with the model equations. This is possible thanks to the nature of the free-radical polymerization, in which the lifetime of a live polymer chain is very short compared with the time scale of the overall reaction.

For copolymer-composition control the input flow of monomer 1 is considered as manipulated variable, and the mole fraction, Φ_{p_1}, of units of monomer 1 in the instantaneous polymer being formed, is used as controlled output variable. The material balance of monomer 1 is replaced by an algebraic equation that forces the amount of monomer 1 in the reactor, M_1, to be a target value $M_{1_{tar}}$. The resulting algebraic equation is simply:

$$M_1 = M_{1_{tar}}. \tag{2}$$

In order to obtain $M_{1_{tar}}$ from the setpoint Φ_{p_1}, the necessary composition of the monomer mixture in the particles (f_{M_1}) is calculated through the copolymer equation using the setpoint composition in copolymer Φ_{p_1}. Once f_{M_1} is known, the thermodynamic partitioning equations (partition coefficient; see Saldívar et al., 1997) are solved to find the amount of monomer 1 present in the reactor that is necessary to yield f_{M_1} in particles.

For MW control, the manipulated variable is the input flow of the chain transfer agent and the instantaneous quantity to be controlled (Kozub and MacGregor, 1992) is

$$y_2 = \frac{d\lambda_0^{2,0}/dt}{d\lambda_0^{1,0}/dt}\,\mathfrak{M}_{\text{inst}},$$

which is the ratio of the time derivatives of the second chain-length dead polymer moment to the first moment, weighted by the average instantaneous molecular weight of the units being polymerized, $\mathfrak{M}_{\text{inst}}$.

Similarly to the treatment used for composition control, the material balance of CTA is replaced by an implicit algebraic equation that forces the value of T (amount of CTA in the reactor) to satisfy the setpoint value of the property y_{sp_2} (target value of weight-average molecular weight). In this case the final equation is

$$y_2(T) - y_{sp_2} = 0 \tag{3}$$

The explicit form of $y_2(T)$ can be obtained from the lumped version of the righthand side of the derivatives of live polymer moments in Saldívar et al. (1997).

The differential equation for the monomer and CTA balances are not solved to define the corresponding states; instead, they are used to generate the optimal flow of the corresponding species. The equations, obtained from material balances, can be written in a generic condensed form as

$$\frac{dS}{dt} = Q_S^f - R_S, \tag{4}$$

where Q_S^f is the required inflow of a chemical species (monomer or CTA) to satisfy the corresponding constraint, and R_S is the rate of consumption of that chemical species by reactions. The equation is solved for Q_S^f, and the derivative dS/dt can be found internally by an integrator like DDASSL (Brenan et al., 1989) that can handle implicit systems and supplies the time derivative of the algebraic state S.

These ideas can be naturally extended to include in the control scheme other polymer properties as shown by Kozub and MacGregor (1992).

Parameter Estimation and Verification Experiments

Eleven experiments were run to gain familiarity with the system and estimate parameters. Experiments 1–4 were of an exploratory nature, and were run to gain familiarity with the system and find good operating conditions for the reaction. These reactions were run with an equimolar (50/50) initial monomer mixture; two of them (run 1 and its replicate, run 2) are shown in Figure 1 to illustrate the reproducibility obtained. Further experimental details are given in Saldívar (1996). The same kind of conversion–time curves shown in Figure 1 were obtained for the same copolymerization system by Dubé and Penlidis (1995) in bulk polymerization; the two regions observed in the plot are due to the very different reactivity ratios.

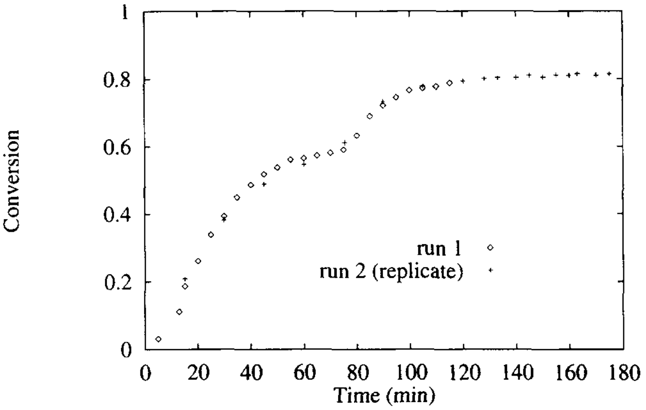

Figure 1. Conversion vs. time curve for a typical exploratory experiment and its replicate.

Experiments 5–11 were run to get estimates of unknown or uncertain parameters for this system. The set of unknown parameters can be classified in four groups: (1) entry-rate coefficients; (2) surfactant isotherm parameters; (3) transfer to CTA rate coefficients; and (4) branching reactions rate coefficients (VAc). The rest of the parameters were available in the literature or could be estimated reasonably well *a priori*. In experiments 5–8 the CTA was charged only at the beginning of the reaction, while the fast-reacting monomer (MMA) was charged in batch or semicontinuous mode; the main characteristics of this set of experiments is listed in Table 2.

Experiments 9 and 10 (and experiment 11, a replicate of 10) were run with input flows of both CTA and MMA. The variety in operating policies was designed to allow for more reliable and robust estimates of the unknown parameters. The formulation for experiments 9–12 is shown in Table 3. Suboptimal flows of monomer and CTA, synthesized with parameter estimates obtained in intermediate stages of the experimental plan, were used in experiments 9–11; the flows utilized in reaction 9 are shown in Figure 2 as illustration. As more experiments were performed, the experimental database for parameter estimation was enriched and the estimates were updated. Further experimental details can be found in Saldívar (1996).

At the end of the parameter-estimation stage, the following conclusions could be drawn: (1) estimates for the first three groups of parameters were obtained; (2) polymer gel was obtained at low to intermediate conversions in the reac-

Table 2. Experimental Design for Parameter Estimation MMA/VAc System

Label	Description
Run 5	Batch, no CTA added
Run 6	Batch, CTA added
Run 7	Semibatch, no CTA added
Run 8	Semibatch, CTA added

Table 3. Formulation for Experiments (9–12)

MMA/VAc g/g	Soap g	Initiator g	CTA g	Solids %
6.0/185	9.23	4.0	4.0	20.0

Table 4. Parameters Used in the Simulations, Runs 7 and 8; Temperature 60°C

Parameter	Value	Units	Reference
Monomer and CTA Partitioning			
A	1.7		Estimated
K_{dw_1}	60		From solubility data*
K_{pw_1}	44		From solubility data*
K_{dw_2}	46.3		From solubility data*
K_{pw_2}	34		From solubility data*
K_T	75		Estimated
Entry/Desorption			
r_m	5.0×10^{-7}	cm	* *
n	2		*
$D_{w1} = D_{p1}$	5.5×10^{-8}	cm²/s	*
$D_{w2} = D_{p2}$	5.5×10^{-8}	cm²/s	Fitted
$m_{d1} = m_{d2}$	1.0		*
$k_{m_{m1}} = k_{p_{m1}}$	1.3×10^{-7}	m/s	Fitted
$k_{m_{m2}} = k_{p_{m2}}$	1.3×10^{-7}	m/s	Fitted
Emulsifier Γ_∞	1.6×10^{-5}	mol/m²	Fitted
Emulsifier b_S	2.0	m³/mol	Fitted
Emulsifier a_{em}	5.0×10^{-20}	m²	Fitted
Emulsifier CMC	1.7×10^{-3}	mol/L	*
Gel Effect			
Gel effect A_5	0.010	L	Fitted
Gel effect A_6	1.808×10^{-1}		Fitted
Gel effect A_7	171.0		Fitted
Physical Properties			
ρ_1	0.919	g/cm³	*
ρ_2	0.932	g/cm³	*
ρ_{p1}	1.19	g/cm³	*
ρ_{p2}	1.17	g/cm³	*

*Rawlings and Ray, 1988.
**Gardon, 1968.

tions; (3) due to lack of suitable equipment, it was not possible to estimate branching reaction rate coefficients; (4) a limiting conversion not predicted by the model was observed in many of the reactions. These points are discussed in more detail below.

Estimates were obtained for entry-rate coefficients, surfactant isotherm parameters, and transfer to CTA-rate coefficients. The parameters obtained at the end of the estimation stage, together with the rest of the parameter values obtained from the literature and used in model calculations, are shown in Tables 4–6 (see also Saldívar and Ray, 1997).

With one set of parameters it was not possible to fit all the data, but this was expected since it is known that for the vinyl acetate/methyl methacrylate system, the effect of composition on the polymerization rate is not well predicted by terminal-unit models. Two different approaches have been used to account for this deficiency of the standard free-radical kinetic theory. It has been suggested (e.g., Ma et al., 1993) that the global rate of polymerization is influenced by the penultimate-unit effect, while a more traditional approach (e.g., Pinto and Ray, 1995), postulates that the effect of composition in reaction rate for this system can be modeled by using a cross-termination Melville ϕ factor (Melville, 1947) that depends on the copolymer composition. In this work an empirical approach is adopted for the model calculations, and two sets of parameters are used for different regions of monomer feed compositions: one for experiments 5 and 6 (equimolar composition in the feed), and one for the rest of the experiments (controlled composition, equimolar composition in the product). This does not represent a problem for the objectives of this work, since under composition control a single set of parameters can be used in a region of small changes in composition.

Experimental data for MW for some of the reactions, together with the model results, are shown in Figure 3. Conversion–time curves from model and experiments, are compared in Figure 4. The mismatch for the limiting conversion for some of the curves is discussed below. The parameters used in the model calculations in Figures 3 and 4 were obtained by fitting data from experiments 9 and 10 only, up to the limiting conversion. The model calculations for experiment 8 were obtained in a purely predictive mode, for which only the trend of the conversion-time curve was correctly predicted.

Most of the polymer samples, especially for experiments 7 and 8, showed gel formation at low to moderate conversion due to terminal double-bond (TDB) and transfer-to-polymer

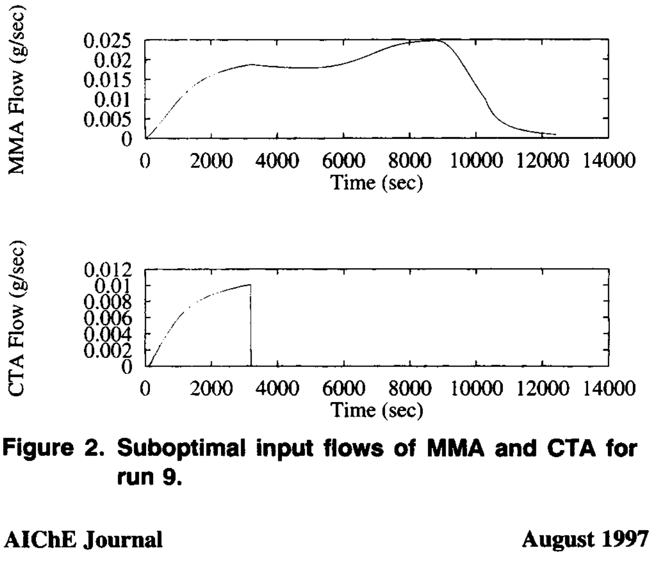

Figure 2. Suboptimal input flows of MMA and CTA for run 9.

Table 5. Kinetic Parameters Used in all Simulations; Temperature 60°C

Parameter	Value	Units	Reference
k_d	7.47×10^{-6}*	s^{-1}	Rawlings and Ray, 1988
f	0.5		Rawlings and Ray, 1988
$k_{p0_{11}}$	600**	L/mol·s	Brandrup and Immergut, 1989
$k_{p0_{22}}$	12,000**	L/mol·s	Brandrup and Immergut, 1989
$k_{t0_{11}}$	3.40×10^{7}*	L/mol·s	Rawlings and Ray, 1988
$k_{t0_{22}}$	2.90×10^{7}	L/mol·s	Odian, 1981
$k_{tr_{11}}$	1.37×10^{-2}*	L/mol·s	Rawlings and Ray, 1988
$k_{tr_{22}}$	2.8**	L/mol·s	Odian, 1981
$k_{tr_{1T}}$	1.05×10^{-1}	L/mol·s	Fitted
$k_{tr_{2T}}$	10.5	L/mol·s	Fitted
r_1	20		Odian, 1981
r_2	0.015		Odian, 1981

*Calculated from an Arrhenius-type expression.
**Middle of the range or average value.

Table 6. Parameters Used in the Simulation of Runs 5 and 6

Parameter	Value	Units
$D_{w2} = D_{p2}$	5.5×10^{-6}	cm^2/s
$k_{m_{m1}} = k_{p_{m1}}$	3.0×10^{-7}	m/s
$k_{m_{m2}} = k_{p_{m2}}$	3.0×10^{-7}	m/s
Γ_∞	2.5×10^{-5}	mol/m^2

reactions (TTP) of vinyl acetate. Up to 30 wt. % of the polymer could not be dissolved in toluene or chloroform. The experimental data shown in Figure 3 correspond to the soluble portion of the polymer; the model calculations in the same figure were obtained having the TTP and TDB reactions inactive. However, in other simulations the model trends showed a maximum in MW at conversions lower than 45% when TTP and TDB reactions were active. The main reason for the occurrence of a maximum in the MW is the balance of effects due to the branching reactions, on the one hand (increasing MW trend), and the decreased monomer concentration in particles when monomer droplets disappear (decreasing MW trend), on the other hand. The monomer droplets disappear at about 32% conversion.

Originally it was planned to obtain estimates for the rate coefficients responsible for branching (TTP and TDB reaction-rate coefficients), by using gel permeation chromatography coupled with a viscometric detector or with a low-angle laser-light-scattering detector; however, none of this equipment was available to us for polymer characterization. Although there are some values reported in the literature for these parameters (Friis et al., 1974; Jang and Lin, 1991; Lee and Mallinson, 1988), they are model-dependent and given as empirical functions of conversion. They were not useful for our model, as they tended to overemphasize the effect of the branching reactions. Given the lack of these coefficients, for the final experiment it was decided that only an optimal flow of MMA would be calculated, *in the presence of a suboptimal CTA flow rate* that would be estimated semiempirically, guided by the model. This would allow us to test the feasibility of achieving the multiobjective optimization in the face of strong interactions of the input variables on the responses.

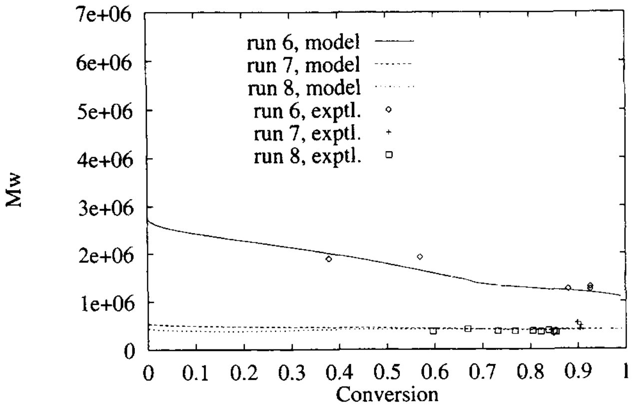

Figure 3. Model and experimental average molecular weight vs. conversion for runs 6-8.

Mark-Houwink coefficients estimated by modified Van Krevelen correlations. The experimental data correspond to the sol fraction of the polymer. The model calculations do not include branching reactions.

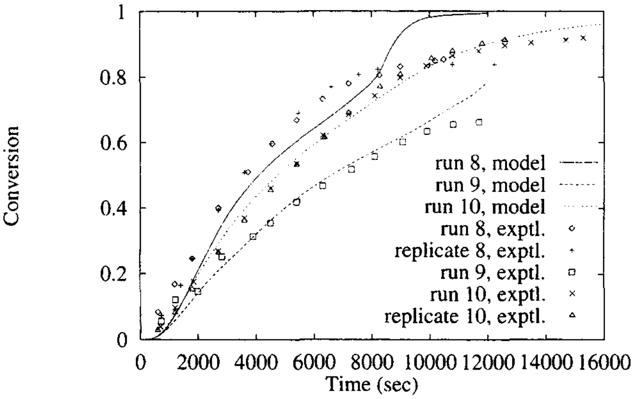

Figure 4. Simulated and experimental conversion vs. time curves for runs 8-11.

The suboptimal flow of CTA was produced by using the simulator and a crude estimate of transfer to polymer rate coefficient (the values tested were 2-10 L/mol·s); this flow was determined based on the requirement that the molecular weight should not grow to the point at which polymer gel would form.

Finally, a verification experiment (run 12) was run with the suboptimal CTA flow designed to avoid gel formation, and an optimal flow of MMA to maintain constant copolymer composition. The corresponding input flows are shown in Figure 5. The experimental conversion-time curve is compared with the model prediction in Figure 6; the agreement is good up to the limiting conversion.

Given this result, the composition control gave excellent results, as expected and illustrated in Figure 7, in which the result from the batch operation with equimolar initial composition is also shown for comparison; the superior performance of the semicontinuous process is obvious.

In the semicontinuous process, with the exception of the point at low conversion, that shows a deviation of 3% with respect to the target, the rest of the (6) points before the limiting conversion show average deviations of 0.3% with respect to the target, which is well within the experimental error of the NMR technique. This is remarkable considering that the large difference in reactivity ratios of the two

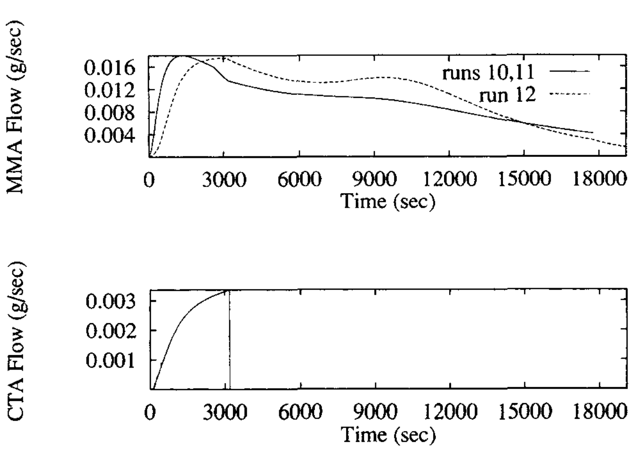

Figure 5. Optimal and suboptimal inputs flows of MMA and CTA, respectively, for reactions 10 and 12.

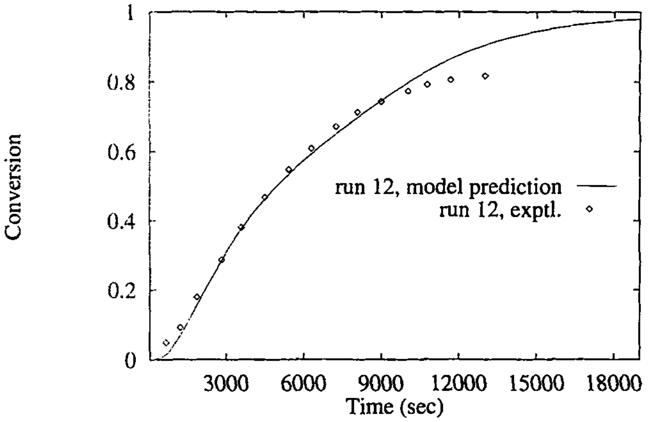

Figure 6. Model prediction and experimental conversion vs. time curves for run 12.

monomers tends to make the composition results very sensitive to modeling and experimental errors.

The last two points after the limiting conversion show important deviations from the target composition because the model did not adequately predict the effects of the limiting conversion on composition. If we can achieve a better mechanistic understanding of the limiting conversion phenomenon, the model can correctly predict the rate of polymerization in this region and the open-loop policy can attempt to control composition to higher conversion. We analyze the question of limiting conversion in the next section.

Finally, in Figure 8, the molecular weights obtained in reaction 12 are shown. The data are nearly constant as desired, except for the point at the lowest conversion, which seems to indicate that the flow of CTA needed to prevent gel formation lowered MW below the target value.

Limiting conversion

After analyzing the experimental conversion and composition data of reaction 12 (no modeling assumptions made), it was concluded that *only the VAc monomer presents a limiting conversion.* This is observed *for VAc monomer only* at about 72–75% of the total conversion. The final increase in conversion observed experimentally (from 75% to 82%) is due to a large extent to polymerization of the MMA fed in the corresponding time period. From a practical point of view, this means that, unless a way is found to avoid a limiting conversion of the VAc monomer, the process should be stopped at 75% conversion, since after that point the achievement of constant-composition copolymer would be extremely slow and eventually impossible. Up to that practical limit, the process used in reaction 12 produced constant-composition copolymer, confirming the feasibility of the techniques used.

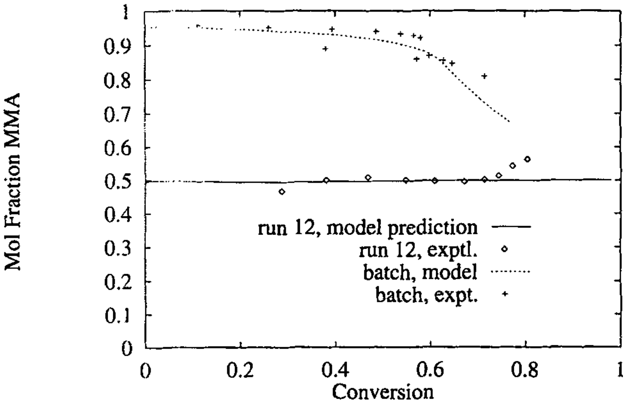

Figure 7. Model and experimental (^{1}H-NMR) MMA molar fraction in polymer vs. conversion for run 12 and for a batch reaction with equimolar monomer feed.

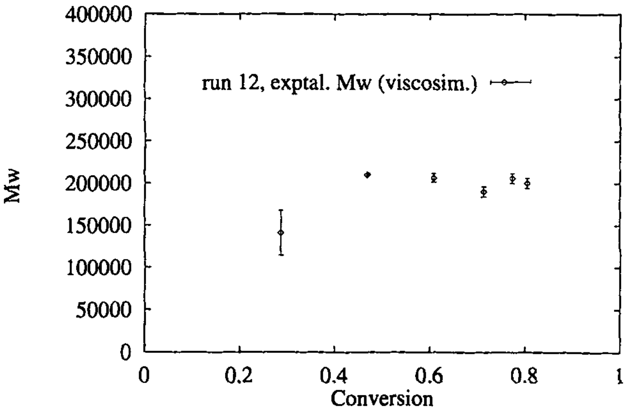

Figure 8. Average molecular weight (±2σ) from viscometric measurements vs. conversion for run 12.

Mark-Houwink coefficients estimated by modified Van Krevelen correlations.

To explain this limiting conversion by modeling, it was decided to run a simulation of reaction 12 in which the partition coefficient of polymer-aqueous phase was decreased, only for VAc monomer, in the region in which an apparent limiting conversion was observed. Simulation results with the modified model are shown in Figure 9. Good agreement is obtained for the composition vs. conversion curve and for the conversion vs. time data, which seems to validate the assumption that the VAc monomer is the only one exhibiting a limiting conversion.

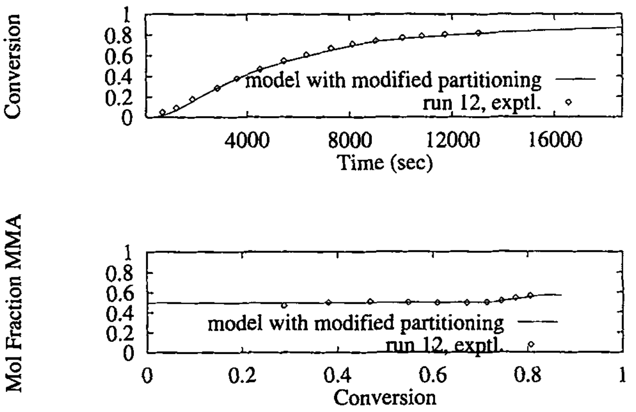

Figure 9. Conversion vs. time and polymer composition vs. conversion for run 12.

Experimental data and model with modified VAc partition coefficient.

From the fundamental point of view, the more likely explanation for the limiting conversion is of a thermodynamic nature and assumes that the transport of VAc from aqueous phase to the particles is considerably hindered due to a reduced driving force as the reaction progresses. Diffusion limitations are easily neglected based on order-of-magnitude calculations. The thermodynamic explanation requires that the amount of VAc present in the reactor when its limiting conversion is reached, is held by the aqueous phase. For reaction 12 this yields a solubility of VAc in water at 60°C of about 4%, which can be compared with a value of 3.5% measured at room temperature for the same system (Zhang, 1996). Also, it is necessary to account for the rather sudden decrease in the partition coefficient of the VAc. A possibility is that the partitioning of the monomer between the aqueous phase and the particles is strongly dependent on the region of the phase diagram in which the system is located. For this theory to be correct, a significant change in the partitioning should be observed in the phase diagram when the system moves from a region of relatively abundant monomer and little polymer, to a region richer in polymer and with relatively little monomer. Sudden changes of this sort have recently been explained (Luna-Bárcenas et al., 1996) with Monte Carlo simulation in terms of entropic contributions, although for our system enthalpic contributions should be even more significant, since it is expected that the interactions between each monomer and the polymer are different.

At the moment there is no conclusive evidence that the partitioning of VAc indeed changes in the way suggested here. Carefully designed experiments for measuring the thermodynamic partitioning of monomer in the region of interest should provide further confirmation or rejection of these ideas.

Nonlinear Model-Predictive Control Scheme

In this section we address the problem of the efficient on-line recomputation of optimal trajectories in the face of errors in the initial conditions and in the presence of disturbances. To that end, we assume that sufficient measurements are available on-line and that they can be used to rebuild the states of the system through on-line estimation. The main innovation in the nonlinear MPC scheme presented here is the way in which the optimization step is handled. In previous nonlinear MPC schemes this step is the most difficult one and is computationally expensive. Looking at previously published work in this field, in an early study of nonlinear MPC, Economou et al. (1986) used an operational formulation to pose the optimization problem. An iterative Newton method, in which the input variable value was assumed constant during the sampling period, was used to calculate the optimal value of the manipulated variable. More recently, Eaton and Rawlings (1992) formulated the optimization step as a full nonlinear optimization problem and solved it using a quadratic programming algorithm. This approach may be computationally difficult to apply for the problem at hand (having around 20 states).

Nonlinear MPC scheme

As in the case of open-loop control synthesis, in order to control the copolymer composition the mole fraction of monomer 1 in the instantaneous polymer being formed, Φ_{p_1}, is used as controlled output variable, and for MW control the instantaneous output variable to be controlled is

$$y_2 = \frac{d\lambda_0^{2,0}/dt}{d\lambda_0^{1,0}/dt}\,\mathcal{M}_{\text{inst}}.$$

The manipulated variables selected are the input flow of monomer 1 and the input flow of the chain-transfer agent.

The MPC algorithm proposed is as follows:

1. At the beginning of a sample interval available measurements are taken and the current states are estimated, as are the present output values.
2. Given the present output values (which may deviate from the setpoint values), the vector of inputs $\boldsymbol{u}(t)$ is calculated for the whole interval between samples, such that the output is forced to follow a linear trajectory from the deviated values to the (constant) vector of setpoints and then stays there. The slope of the linear trajectory is based on a user-specified correction time Δt. Mathematically, the linear trajectory for each output is represented by the following equation (see Figure 10):

$$\begin{aligned} y_{tt_i} &= y_{0_i} + \frac{y_{sp_i} - y_{0_i}}{\Delta t_i}(t - t_{0_i}) \\ & t_{0_i} \le t \le \min\{t_{0_i} + \Delta t_i,\ t_{0_i} + \Delta\Theta_i\} \\ y_{tt_i} &= y_{sp_i} \quad \min\{t_{0_i} + \Delta t_i,\ t_{0_i} + \Delta\Theta_i\} \le t, \end{aligned} \tag{5}$$

where y_{tt_i} is the (moving) temporary target value of the ith output variable at the current time t; y_{0_i} is the value of the output variable i at the beginning of its corresponding sampling interval $\Delta\Theta_i$ that started at time t_{0_i}; y_{sp_i} is the constant setpoint value for the ith output; and Δt_i is the time period in which the correction is desired to take place. The calculation of the required input vector $\boldsymbol{u}(t)$ implies an inversion of the model of the plant and is based again on the instantaneous property method. The inversion is accomplished by solving a system of differential-algebraic equations consisting of the equations of the model in which the material balances for the manipulated variables have been replaced by the following set of algebraic equations:

$$y_{tt_i} = h_i(\boldsymbol{u}, \boldsymbol{x}), \tag{6}$$

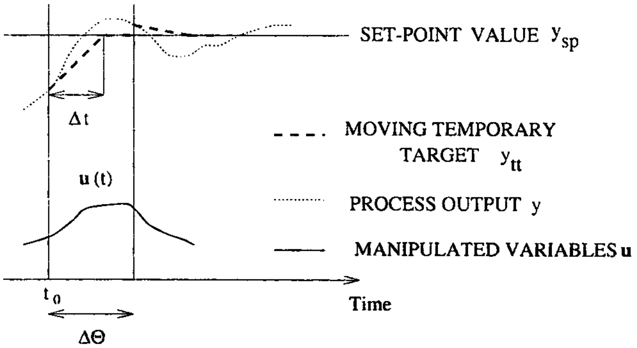

Figure 10. Elements of the MPC scheme.

where y_{tt_i} is the value specified by Eq. 5, and h_i defines the instantaneous ith output in terms of the input $\boldsymbol{u}$ and the vector of states $\boldsymbol{x}$. The functions h_i are defined by the same set of relationships described for the calculations of optimal open-loop trajectories.

3. When a new sample is taken, the process is repeated.

The scheme gradually changes the effective target value (moving temporary target) from the value of the output variable at the beginning of the sampling interval, to the constant desired setpoint at the end of the correction time. Once the setpoint is reached, the temporary target coincides with the setpoint. The vector of inputs $\boldsymbol{u}(t)$ is a function of time during the sampling period.

In terms of tuning parameters, the shorter the correction time Δt_i, the more aggressive the action of the controller. Ideally, the correction time Δt_i should be shorter or equal to the sampling period $\Delta\Theta_i$.

Test simulations

In order to test the nonlinear MPC scheme by simulation, the same system used throughout this article has been selected for illustration. The set of parameters used for these simulations is very similar to those used for the experimental verification of open-loop policies; the complete set of parameters is given in Saldívar (1996).

From preliminary simulations an additional issue was found: in order to use the CTA as a manipulated variable to control the MW, the process has to satisfy the condition that, in the absence of the semicontinuous flow of CTA, the MW should exhibit an increasing trend for most of the polymerization. Only in this way can the flow of CTA necessary to maintain a constant MW be positive, since the only two mechanisms for reducing the concentration of CTA in the reactor, dilution effect and consumption of CTA by reactions, may not be large enough. Exploratory simulations showed that for a simple semicontinuous process the MW exhibited an initially decreasing trend that would have required a negative flow of CTA to maintain constant MW. In order to obtain an increasing MW at early reaction stages, the former process was modified so only a fraction of the slow monomer (VAc) would be charged at time zero, while the rest would be charged during the initial minutes of the polymerization at a prespecified flow rate. Since some CTA is present in the reactor at time zero, the addition of monomer would increase the dilution effect on the CTA in the whole of the organic phase, leading to an increasing trend in the MW and requiring a positive inflow of CTA to counterbalance that trend. The faster the monomer addition rate, the steeper the positive slope of MW vs. time. Once the transfer to polymer reactions becomes important, the increasing trend of the MW will continue by virtue of them. This is true for most of the reaction (up to 70–80% conversion); however, at some high conversion, and even in the presence of TTP reactions, the MW reaches a maximum and then decreases.

The process design utilized for testing the MPC scheme is as follows:

- A fraction (20–40%) of the slow monomer (VAc) is charged to the reactor at time zero. The necessary amount of the fast monomer (MMA) for the desired copolymer composition setpoint (50/50 molar) is also initially charged, as is the necessary amount of the CTA to obtain at time zero the desired MW. The exact required amounts can be calculated by solving a system of algebraic equations at initial conditions. All the water, initiator, and emulsifier are also added at time zero.
- The rest of the slow monomer is added at a prespecified flow rate during some period of time (5–50 min) at the beginning of the reaction.
- The nominal input flows of the fast monomer and the CTA are given by the open-loop optimal policies.

All the simulations were run until a limiting conversion (93–94%) predicted by the glass-effect model was reached. The operation was assumed isothermal at 50°C.

For the model solution, the integrator DASRT (Brenan et al., 1989) was employed, together with initial conditions (at time zero and restart points) provided by the algebraic solver NLEQ (Nowak and Weimann, 1990). Each calculation started with the plant simulated until a measurement was available. At that point, and using the assumption of state estimates available, the optimization would be run for the next sampling time interval, using as initial conditions for the model the last values provided by the plant simulation. The recomputed optimal input flows were then used to simulate the plant behavior for the just-calculated time interval. When during the optimization calculations a persistent negative flow of CTA was required, the CTA flow was set to zero and only the composition was optimized. This occurred usually at about 70–80% conversion and explains why the MW decreases in the last stage in the MPC-controlled cases. All the simulations took 3–4 min on a DEC 3000-600 workstation.

Numerical example

In this case the initial amount of monomer 2 was assumed to be 20% of its final total, and the remaining 80% was charged to the reactor at a constant flow rate Q_2^f in the initial 400 s. The rest of the operating conditions simulated can be found in Saldívar (1996). The target values for the controlled variables were MW = 477,000 and $\Phi_{p_1} = 0.5$. The disturbance studied in this case was an error of +40% in Q_2^f. Figure 11 shows a comparison of the system responses for cumulative and instantaneous MW, when only open-loop optimal control is used and when the MPC control corrections

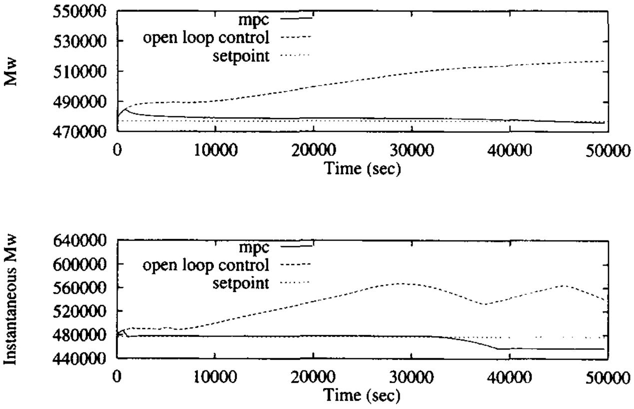

Figure 11. Molecular-weight responses with no control and with MPC, to a disturbance of +40% in Q_2^f.

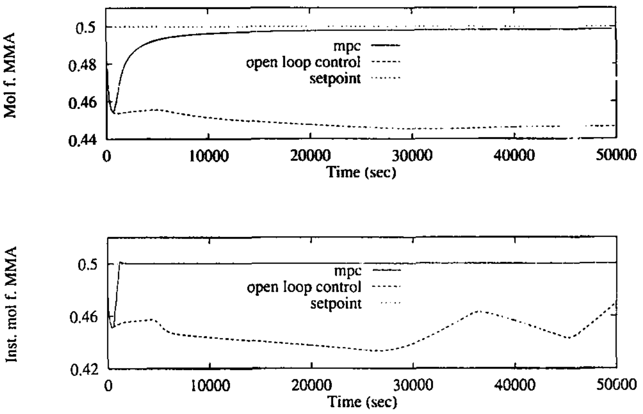

Figure 12. Copolymer-composition responses with no control and with MPC, to a disturbance of +40% in Q_2^f.

are applied, with measurements/estimations every 600 s and tuning parameters $\Delta t_{MW} = 600$ and $\Delta t_\Phi = 600$. The MPC controller shows excellent performance, especially when judged by the instantaneous polymer MW evolution. Judging from the plot of cumulative MW, it would seem that this property does not deteriorate significantly when only open-loop control is applied; however, by looking at the instantaneous property behavior, one realizes that the instantaneous MW shows deviations of up to 100,000 units in the instantaneous polymer produced and, more importantly, that on-target polymer is not produced in a significant amount when open-loop control is applied. Thus, for close control of MW, the MPC performs well.

A similar situation is observed for the same simulations in Figure 12, in which the cumulative and instantaneous molar fraction of MMA are plotted. In this case both the instantaneous and cumulative properties show large deviations (at least 5%) from the target when uncorrected open-loop control is used. Notice that the MPC is designed such that the composition control is maintained even when the MW control is disabled due to input constraints. The composition control is excellent, as shown by the instantaneous copolymer composition response.

Additional examples and simulations for a number of disturbances in monomer, CTA, and emulsifier are available in Saldívar (1996). A single set of controller parameters (the correction times Δt_i) were able to handle well all these cases.

Concluding Remarks

In this article, a general methodology that can be used in industry was presented to design control policies for semicontinuous emulsion polymerization processes that will produce polymers with properties satisfying multiple objectives. The methodology was introduced by using, as an example, the problem of synthesizing optimal policies to produce a copolymer with constant composition and constant molecular weight, but the concepts and techniques presented here are not restricted by the number of properties at hand or the reference trajectories pursued (as long as these are smooth).

The philosophy behind the methodology presented in this article is that a general mathematical model, with a minimum number of adjustable parameters, can be used to generate optimal open-loop policies. The unknown parameters, which have a clear physical meaning, can be estimated through a few experiments and be finely tuned in the region around the conditions of interest. In the experimental section it was shown how this procedure resulted in quantitative predictive power for conversion rate and copolymer composition, and how this allowed for accurate control of composition. The mathematical synthesis of the optimal open-loop policies is based on the optimization of properties of the instantaneous polymer being formed, a technique that presents clear advantages over more involved mathematical optimization procedures.

Rough estimates of the parameters related to the evolution of MW were obtained, and therefore only suboptimal policies were tested in conjunction with the optimal policies used for the composition control. This showed how a global approach, based on a general model, allows one to deal effectively with multivariable control problems in which strong interactions between input and output variables are present. The experimental results presented here point out the feasibility of application of the methodology outlined in this article.

To our knowledge this is the first work addressing experimentally the important problem of tailoring multiple outputs in emulsion copolymerization. Although only one composition was selected to illustrate the feasibility of the proposed techniques, the experimental verification performed is a stringent test of the methodology presented, due to the fact that this selection was arbitrary and that the composition control of this system is a challenging task. In order to make the application more realistic, unseeded polymerizations were used. It was also found that rate coefficients for branching reactions can play a significant role in the successful experimental application of these optimization techniques.

Finally, a nonlinear MPC scheme for on-line optimization of polymer properties was introduced and tested by simulation. This scheme naturally exploits the efficiency and simplicity of optimal open-loop policies based on the control of instantaneous polymer properties. When tested by simulation, the scheme showed excellent performance in handling disturbances, under the assumption that the states can be estimated on-line. Further investigation of this scheme and of the associated problems related to its implementation, such as on-line state and parameter estimation, are topics of future research.

Notation

b_S = parameter in adsorption isotherm for surfactant
cmc = critical micelle concentration of surfactant
f = feed (subscript)
k_d = rate constant for thermal decomposition of initiator
$k_{m_{mi}}$ = mass-transfer coefficient for type i radical entering micelles
$k_{m_{pi}}$ = mass-transfer coefficient for type i radical entering particles
$k_{t0_{ij}}$ = rate constant for total termination between radicals of types i and j
$k_{tr_{ij}}$ = rate constant for chain transfer of type i radical to monomer j
$k_{tr_{iT}}$ = rate constant for chain transfer of type i radical to chain transfer agent
$k^w_{tr_{ij}}$ = rate constant for chain transfer of type i radical to monomer j in aqueous phase
M_w = weight average molecular weight
n = exponent of radius for entry rate expression
N_A = Avogadro's number

r_i = reactivity ratio, monomer i
r_m = radius of a micelle
V_w = volume of water in reactor
Γ_∞ = parameter in adsorption isotherm for surfactant
$[\eta]$ = intrinsic viscosity
ρ_i = density of component i

Literature Cited

Araujo, O., “Copolymerization and Terpolymerization in Emulsion: Experimental Work and Study of Issues Related to the Mathematical Modeling of the Process,” PhD Thesis (in Portuguese), Escola Politécnica de Univ. de São Paulo, Brazil (1997).

Arzamendi, G., and J. M. Asúa, “Monomer Addition Policies for Copolymer Composition Control in Semicontinuous Emulsion Copolymerization,” *J. Appl. Poly. Sci.*, **38**, 2019 (1989).

Arzamendi, G., and J. M. Asúa, “Copolymer Composition Control During the Seeded Emulsion Copolymerization of Vinyl Acetate and Methyl Acrylate,” *Makromol. Chem., Macromol. Symp.*, **35/36**, 249 (1990).

Arzamendi, G., J. R. Leiza, and J. M. Asúa, “Semicontinuous Emulsion Copolymerization of Methyl Methacrylate and Ethyl Acrylate,” *J. Poly. Sci., Part A: Poly. Chem.*, **29**, 1549 (1991).

Bassett, D. R., and K. L. Hoy, “Nonuniform Emulsion Polymers,” *Emulsion Polymers and Emulsion Polymerization*, Chap. 23, D. R. Bassett and A. E. Hamielec, eds., *ACS Symp. Ser. 165*, p. 371 (1981).

Brandrup, J., and E. H. Immergut, *Polymer Handbook*, 3rd ed., Wiley, New York (1989).

Brenan, K. E., S. L. Campbell, and L. R. Petzold, *Numerical Solution of Initial Value Problems in Differential Algebraic Equations*, Elsevier/North-Holland, New York (1989).

Broadhead, T. O., A. E. Hamielec, and J. F. MacGregor, “Dynamic Modelling of the Batch, Semibatch and Continuous Production of Styrene/Butadiene Copolymers by Emulsion Polymerization,” *Makromol. Chem., Suppl.*, **10/11**, 105 (1985).

Canegallo, S., P. Canu, M. Morbidelli, and G. Storti, “Composition Control in Emulsion Copolymerization. II. Application to Binary and Ternary Systems,” *J. Appl. Poly. Sci.*, **54**, 1919 (1994).

Canu, P., S. Canegallo, M. Morbidelli, and G. Storti, “Composition Control in Emulsion Copolymerization. I. Optimal Monomer Feed Policies,” *J. Appl. Poly. Sci.*, **54**, 1899 (1994).

Choi, K. Y., and D. N. Butala, “An Experimental Study of Multiobjective Dynamic Optimization of a Semibatch Copolymerization Process,” *Poly. Eng. Sci.*, **31**, 353 (1991).

Chujo, K., Y. Harada, S. Tokuhara, and K. Tanaka, “The Effects of Various Monomer Addition Methods on the Emulsion Copolymerization of Vinyl Acetate and Butyl Acrylate,” *J. Poly. Sci., Part C*, **27**, 321 (1969).

Congalidis, J. P., J. R. Richards, and W. H. Ray, “Feedforward and Feedback Control of a Solution Copolymerization Reactor,” *AIChE J.*, **35**, 891 (1989).

Dimitratos, J., C. Georgakis, M. S. El-Aasser, and A. Klein, “Dynamic Modeling and State Estimation for an Emulsion Copolymerization Reactor,” *Comput. Chem. Eng.*, **13**(1/2), 21 (1989).

Dimitratos, J., C. Georgakis, M. S. El-Aasser, and A. Klein, “An Experimental Study of Adaptive Kalman Filtering in Emulsion Copolymerization,” *Chem. Eng. Sci.*, **46**(12), 3203 (1991).

Dubé, M. A., and A. Penlidis, “A Systematic Approach to the Study of Multicomponent Polymerization Kinetics—The Butyl Acrylate/Methyl Methacrylate/Vinyl Acetate Example: 1. Bulk Copolymerization,” *Polymer*, **36**(3), 587 (1995).

Eaton, J. W., and J. B. Rawlings, “Model Predictive Control of Chemical Processes,” *Chem. Eng. Sci.*, **47**(4), 705 (1992).

Economou, C. G., M. Morari, and B. O. Palsson, “Internal Model Control. 5. Extension to Nonlinear Systems,” *Ind. Eng. Chem. Process Des. Dev.*, **25**, 403 (1986).

El-Aasser, M. S., T. Makgawinata, J. W. Vanderhoff, and C. Pichot, “Batch and Semicontinuous Emulsion Copolymerization of Vinyl Acetate and Butyl Acrylate: I. Bulk, Surface and Colloidal Properties of Copolymer Latexes,” *J. Poly. Sci., Poly. Chem. Ed.*, 21, 2363 (1983).

Friis, N., D. Goosney, J. D. Wright, and A. E. Hamielec, “Molecular Weight and Branching Development in Vinyl Acetate Emulsion Polymerization,” *J. Appl. Poly. Sci.*, **18**, 1247 (1974).

Gagnon, L., and J. F. MacGregor, “State Estimation for Continuous Emulsion Polymerization,” *Can. J. Chem. Eng.*, **69**, 648 (1991).

Gardon, J. L., “Emulsion Polymerization: I. Recalculation and Extension of the Smith-Ewart Theory,” *J. Poly. Sci., Part A-1*, **6**, 623 (1968).

Guillot, J., “A Thermodynamic Approach to Emulsion Copolymerization,” *Makromol. Chem., Rapid Commun.*, **1**, 697 (1980).

Guyot, A., J. Guillot, C. Pichot, and L. Ríos, “New Design for Producing Constant Composition Copolymers in Emulsion Polymerization,” *Emulsion Polymers and Emulsion Polymerization*, Chap. 26, D. R. Bassett and A. E. Hamielec, eds., *ACS Symp. Ser. 165*, p. 415 (1981).

Hanna, R. J., “Synthesis of Chemically Uniform Copolymers,” *Ind. Eng. Chem.*, **49**, 208 (1957).

Hicks, J. A., A. Mohan, and W. H. Ray, “The Optimal Control of Polymerization Reactors,” *Can. J. Chem. Eng.*, **47**, 590 (1969).

Jang, S., and P. Lin, “Discontinuous Minimum End-Time Temperature/Initiator Policies for Batch Emulsion Polymerization of Vinyl Acetate,” *Chem. Eng. Sci.*, **46**(12), 3153 (1991).

Kozub, D. J., and J. F. MacGregor, “Feedback Control of Polymer Quality in Semibatch Copolymerization Reactors,” *Chem. Eng. Sci.*, **47**(4), 929 (1992).

Lee, C. H., and R. G. Mallison, “A Model for Molecular Weights in Vinyl Acetate Emulsion Polymerization,” *AIChE J.*, **34**(5), 840 (1988).

Leiza, J. R., J. C. de la Cal, G. R. Meira, and J. M. Asúa, “On-Line Copolymer Composition Control in the Semicontinuous Emulsion Copolymerization of Ethyl Acrylate and Methyl Methacrylate,” *Poly. Reac. Eng.*, **1**(4), 461 (1992–1993).

Luna-Barcenas, G., G. E. Bennet, I. C. Sánchez, and K. F. Johnston, “Monte Carlo Simulation of Polymer Chain Collapse in Athermal Solvents,” *J. Chem. Phys.*, **104**, 9971 (1996).

Ma, Y., Y. Won, K. Kubo, and T. Fukuda, “Propagation and Termination Processes in the Free-radical Copolymerization of Methyl Methacrylate and Vinyl Acetate,” *Macromolecules*, **26**, 6766 (1993).

Melville, H. W., B. Noble, and W. F. Watson, “Copolymerization. I. Kinetics and Some Experimental Considerations of a General Theory,” *J. Poly. Sci.*, **2**, 229 (1947).

Nowak, U., and L. Weimann, “A Family of Newton Codes for Systems of Highly Nonlinear Equations—Algorithm, Implementation, Application,” ZIB (Konrad Zuse Zentrum fuer Informationstechnik Berlin), Tech. Rep. TR 90-10 (1990).

Odian, G., *Principles of Polymerization*, 2nd ed., Wiley, New York (1981).

O'Toole, J. T., “Kinetics of Emulsion Polymerization,” *J. Appl. Poly. Sci.*, **9**, 1291 (1965).

Pinto, J. C., and W. H. Ray, “The Dynamic Behavior of Continuous Solution Polymerization Reactors VII. Experimental Study of a Copolymerization Reactor,” *Chem. Eng. Sci.*, **50**, 715 (1995).

Rawlings, J. B., and W. H. Ray, “The Modelling of Batch and Continuous Emulsion Polymerization Reactors: II. Comparison with Experimental Data from Continuous Stirred Tank Reactors,” *Polym. Eng. Sci.*, **28**(5), 257 (1988).

Ray, W. H., *Advanced Process Control*, Butterworths, Boston (1989).

Ríos, L., M. A. Cruz, J. Palacios, L. M. Ruiz, and A. García-Rejón, “Batch and Semicontinuous Emulsion Copolymerization Styrene/Methyl Methacrylate: Kinetics and Viscoelastic Properties,” *Makromol. Chem. Suppl.*, **10/11**, 477 (1985).

Sacks, M. E., S. Lee, and J. A. Biesenberger, “Effect of Temperature Variations on Molecular Weight Distributions: Batch, Chain Addition Polymerizations,” *Chem. Eng. Sci.*, **28**, 241 (1973).

Saldívar, E., “Modeling and Control of Emulsion Copolymerization Reactors,” PhD Thesis, University of Wisconsin, Madison (1996).

Saldívar, E., P. Dafniotis, and W. H. Ray, “Detailed Modeling of Emulsion Copolymerization Reactors: I. Application to Reactors Operating above the CMC of the Emulsifier, 1997,” *J. Macromol. Sci.-Rev. Macromol. Chem. Phys.*, in press (1997).

Saldívar, E., and W. H. Ray, “Mathematical Modeling of Emulsion Copolymerization Reactors. Experiment Validation and Application to Complex Systems,” *Ind. Eng. Chem. Res.*, **36**(4), 1322 (1997).

Thomas, I. M., and C. Kiparissides, “Computation of the Near-optimal Temperature and Initiator Policies for a Batch Polymerization Reactor,” *Can. J. Chem. Eng.*, **62**, 284 (1984).

Tsoukas, A., M. Tirrell, and G. Stephanopoulos, "Multiobjective Dynamic Optimization of Semibatch Copolymerization Reactors," *Chem. Eng. Sci.*, **37**(12), 1785 (1982).

van Doremaele, G. H. J., H. A. S. Schoonbrood, J. Kurja, and A. L. German, "Copolymer Composition Control by Means of Semicontinuous Emulsion Copolymerization," *J. Appl. Poly. Sci.*, **45**, 957 (1992).

Van Krevelen, D. W., *Properties of Polymers*, 3rd ed., Elsevier, New York (1990).

Zhang, S. X., "Modeling and Experimental Studies of Free-radical Polymerization Reactors," PhD Thesis, Univ. of Wisconsin, Madison (1996).

Appendix: Summary of Mathematical Model

Particle-size distribution

$$\frac{dF(t)V_w}{dt} = V_{aq}N_A\left(\sum_{i=1}^{c} a_m k_{m_{mi}} M[P_i]_w + a_m k_{m_{mR}} M[R]_w\right) \tag{A1}$$

with initial condition

$$F(t=0) = F_0, \tag{A2}$$

where $F(t)$ is the total number of particles per unit volume of water at time t; V_w and V_{aq} are the volumes of water and aqueous phase (solubilized material included), respectively; N_A is the Avogadro number; c is the number of different types of monomers; a_m is the surface area of a micelle; and M is the micelle concentration. The $k_{m_{mi}}$ and $k_{m_{mR}}$ are entry rate coefficients for type i radicals with aqueous phase concentration $[P_i]_w$ and initiator radicals with aqueous phase concentration $[R]_w$, respectively.

Desorption coefficient for radicals in particles

$$de_i = g_i \frac{K_{0i}}{K_{0i} + \sum_{j=1}^{c} k_{p_{ij}}[M_j]_p} \quad i = 1, \ldots, c, T \tag{A3}$$

$$K_{0i} = \frac{12}{d_p^2}\frac{D_{wi}D_{pi}}{m_{di}D_{pi} + 2D_{wi}}, \tag{A4}$$

where g_i is the frequency of generation (rate per total radicals) of monomeric radicals of type i from a particle; $k_{p_{ij}}$ is the propagation rate constant of a type i radical with a monomer j; and $[M_j]_p$ is the concentration of monomer j in particles; d_p is the diameter of the particle; D_{wi} and D_{pi} are the diffusion coefficients of monomeric radicals in the aqueous phase and in particles, respectively; and m_{di} is a partition coefficient between the aqueous and the particle phase for monomer i or CTA.

Average number of radicals in particles

Given as an algebraic relationship in terms of Bessel functions from the classic solution to the Smith–Ewart equation by Stockmayer and O'Toole (O'Toole, 1965).

Species balances

Monomer balances and polymer balances for c components represented by $2c$ ODEs. Balances for initiator, surfactant, CTA, inhibitor, water, and total reaction mass are represented by one ODE each. The distribution of radical types yields one linear system of dimension c for each one of the phases: particles and aqueous phase. The aqueous-phase radical balance at QSSA gives only one nonlinear algebraic equation for the total aqueous-phase radical amount. Other aqueous-phase balances for different polymeric radicals (primary, monomeric, and critical length) under the QSSA, are given in terms of explicit algebraic relationships.

Monomer partitioning: Partition coefficients

Although more sophisticated thermodynamic models are available in the literature (c.f. Guillot, 1980), it was decided to use a simple one in order to maintain simplicity and robustness for potential on-line application:

$$K_{dw_i} = \frac{[M_i]_d^m}{[M_i]_w^m} \quad i = 1, \ldots, c \tag{A5}$$

$$K_{pw_i} = \frac{[M_i]_p^m}{[M_i]_w^m} \quad i = 1, \ldots, c, \tag{A6}$$

where $[M_i]_d^m$, $[M_i]_w^m$, and $[M_i]_p^m$ are mass-basis concentration of monomer in droplets, aqueous phase, and particle phase, respectively. Polymer swelling is defined as

$$\frac{V_p \sum_{i=1}^{c} [M_i]_p^m}{P} = A, \tag{A7}$$

where V_p is volume of particles, P is the total amount of polymer in particles in mass basis, and A is an empirical constant. Monomer partitioning yields a nonlinear algebraic system of dimension 3.

CTA partitioning: Partition coefficient

$$K_T = \frac{[T]_o}{[T]_{aq}}, \tag{A8}$$

where $[T]_o$ and $[T]_{aq}$ are concentration of CTA in organic phases (droplets and particles) and in the aqueous phase, respectively.

Surfactant equilibrium

Surfactant adsorbed onto particles represented by a Langmuir-type adsorption isotherm

$$S_a = \frac{S_p\Gamma_\infty b_s S_F/V_{aq}}{1 + b_s S_F/V_{aq}}, \tag{A9}$$

where S_p is the total surface area of particles; S_F is the free surfactant in the aqueous phase; and Γ_∞ and b_s are parameters.

Micelle concentration M

$$M' = \frac{([S]_w - [S]_w^{cmc}) N_A a_{em}}{a_m} \tag{A10}$$

$$M = M' H(M'), \tag{A11}$$

where $[S]_w$ is the concentration of surfactant in the aqueous phase; $[S]_w^{cmc}$ is the critical micelle concentration of the surfactant; a_{em} is the area of a micelle covered by a molecule of surfactant; and H is the Heaviside or unit step function.

Molecular-weight distribution: Moments of live polymer

Moments of live polymer with respect to chain length and number of branches are defined as

$$\mu_n^{G,H}(t) = \sum_{l=0}^{\infty} \sum_{b=0}^{\infty} \sum_{n=1}^{\infty} l^G b^H N_n^{l,b}(t), \tag{A12}$$

and total moments of live polymer with respect to chain length, number of branches, and number of radicals in particle are defined as

$$\mu_S^{G,H}(t) = \sum_{l=0}^{\infty} \sum_{b=0}^{\infty} \sum_{n=1}^{\infty} l^G b^H n^S N_n^{l,b}(t), \tag{A13}$$

where $N_n^{l,b}(t)$ is the number of growing radicals of length l and branching index b present per liter of water in particles having n live radicals at time t. Capital letters are used to denote the order of the moments over the corresponding variable. The lumped population balance equation for live polymer (using the QSSA) results in

$$\frac{d\mu_n^{G,H}(t) V_w}{dt} = \sum_{j=1}^{\text{Mech}} r_j \approx 0$$

$$G, H = 0, \ldots, \infty \qquad n = 1, \ldots, \infty. \tag{A14}$$

The terms r_j on the righthand side correspond to the different mechanisms that change the classification of radicals, including all the chemical reactions as well as other physicochemical phenomena such as entry and desorption of radicals. A complex free-radical kinetic scheme has been modeled that includes chain transfer to polymer, terminal and internal double-bond polymerization, scission, inhibition, and reverse propagation, in addition to the traditional free-radical kinetic scheme with initiation, propagation, termination, and chain transfer to monomer and to chain transfer agent.

Molecular-weight distribution: Moments of dead and bulk polymer

Moments of dead polymer are defined as

$$\lambda_S^{G,H}(t) = \sum_{l=0}^{\infty} \sum_{b=0}^{\infty} \sum_{n=0}^{\infty} l^G b^H n^S D_n^{l,b}(t), \tag{A15}$$

where $D_n^{l,b}(t)$ is the number of dead polymer chains of length l and branching index b present per liter of water in particles having n live radicals at time t.

Moments of bulk polymer are defined by

$$\Omega_S^{G,H} = \lambda_S^{G,H} + \mu_S^{G,H}. \tag{A16}$$

The population balance equation for bulk polymer is

$$\frac{d\Omega_S^{G,H}(t) V_w}{dt} = \sum_{j=1}^{\text{Mech}} r_j$$

$$G, H = 0, \ldots, \infty \qquad n = 1, \ldots, \infty \qquad S = 0, 1, \ldots, \infty. \tag{A17}$$

For estimation of polymer properties only the moments $S = 0$ on number of radicals are required. The MWD is described by the first 3 $\Lambda_0^{G,H}$ moments over chain length (for all possible branches), represented by the values $GH = 00$, $GH = 10$, and $GH = 20$.

Manuscript received Aug. 2, 1996, and revision received Feb. 20, 1997.